Signals from the metastatic niche regulate early and advanced ovarian cancer metastasis through miR-4454 downregulation

Subramanyam Dasari[1], Taruni Pandhiri[1], Tommaso Grassi[2], Daniel W Visscher[3], Francesco Multinu[2], Komal Agarwal[1,4], Andrea Mariani[2], Viji Shridhar[3], Anirban K Mitra[1,5,6*]

1 Medical Sciences Program, Indiana University School of Medicine, Bloomington, IN
2 Department of Obstetrics and Gynecology, Mayo Clinic, Rochester, MN.
3 Department of Laboratory Medicine and Pathology, Mayo Clinic, Rochester, MN
4 Department of Obstetrics and Gynecology, St. Vincent Dunn Hospital, Bedford, IN
5 Department of Medical and Molecular Genetics, Indiana University School of Medicine, Indianapolis, IN
6 Indiana University Melvin and Bren Simon Cancer Center, Indianapolis, IN

Running title: Microenvironmental regulation of OC metastasis via p53 and FAK

Keywords: Metastasis, microRNA, microenvironment, ovarian cancer, miR-4454, fibroblast.

Additional information:
Financial support: AKM was supported by DoD OCRP Ovarian Cancer Academy Award (W81XWH-15-0253), Colleen's Dream Foundation, CTSI core pilot and Ralph W. and Grace M. Showalter Research awards. The tumor collection and miRNAseq was supported in part by the grants from the National Institutes of Health (P50CA136393), Andersen Foundation grant (AM), the Department of Experimental Pathology and Laboratory Medicine, and Mayo Clinic (VS).

***Corresponding author:** Anirban K. Mitra, E-mail: anmitra@indiana.edu. 915 E. 3rd Street, Myers Hall 200C, Bloomington, Indiana 47405. Phone: (812) 856-1207, FAX: (812) 855-4436.

Conflict of interest: The authors have no conflict of interest.

This is the author's manuscript of the article published in final edited form as:

Dasari, S., Pandhiri, T., Grassi, T., Visscher, D. W., Multinu, F., Agarwal, K., Mariani, A., Shridhar, V., & Mitra, A. K. (2020). Signals from the Metastatic Niche Regulate Early and Advanced Ovarian Cancer Metastasis through miR-4454 Downregulation. Molecular Cancer Research: MCR, 18(8), 1202–1217. https://doi.org/10.1158/1541-7786.MCR-19-1162

Abstract

Treatment of ovarian cancer (OC) is limited by extensive metastasis and yet it remains poorly understood. We have studied the critical step of metastatic colonization in the context of the productive interactions with the metastatic microenvironment with a goal of identifying key regulators. By combining microRNA expression analysis using an organotypic 3D culture model of early OC metastasis with that of matched primary and metastatic tumors from 42 OC patients, we identified miR-4454 as a key regulator of both early colonization and advanced metastasis in OC patients. miR-4454 was downregulated in the metastasizing OC cells through paracrine signals from microenvironmental fibroblasts, which promoted migration, invasion, proliferation and clonogenic growth in OC cells as well as their ability to penetrate through the outer layers of the omentum. Stable overexpression of miR-4454 decreased metastasis in OC xenografts. Its mechanism of action was through the upregulation of its targets, secreted protein acidic and cysteine rich (SPARC) and BCL2 associated athanogene 5 (BAG5), which activated focal adhesion kinase (FAK) signaling, promoted mutant p53 gain of function by its stabilization and inhibited apoptosis. Since microenvironment-induced downregulation of miR-4454 is essential for early and advanced metastasis, targeting it could be a promising therapeutic approach.

Implications: This study identifies a microRNA, miR-4454, which is downregulated by signals from the microenvironment and promotes early and advanced OC metastasis through its effects on FAK activation, mutant p53 stabilization and apoptosis inhibition.

Introduction

Most ovarian cancer (OC) patients present with metastasis at the time of diagnosis (1). This contributes towards OC being the deadliest gynecologic malignancy and the fifth leading cause of deaths due to cancer among women (2). The poor outcome stems from our limited understanding of the mechanisms regulating metastasis (3). Metastasis is a multi-step process and metastatic colonization – the final step in the cascade - is considered the rate-limiting step (4). Upon reaching the omentum, the metastasizing OC cells encounter a new microenvironment, consisting of the mesothelium and the underlying basement membrane containing fibroblasts and extracellular matrices (ECMs) (5). To successfully establish the metastatic tumor, the OC cells need to adapt to the new microenvironment and utilize the new set of signaling factors and ECMs. This requires productive reciprocal interactions with the new microenvironment and consequent changes in gene expression.

microRNAs are small non-coding RNAs that can serve as master regulators of gene expression by sequence specific inhibition of translation of many target mRNAs (6,7). microRNAs can pleiotropically regulate multiple steps in cancer progression and can serve oncogenic or tumor suppressor roles (8,9). They have been implicated in the regulation of OC metastasis and reprogramming of the tumor microenvironment (7,9-11). We have previously reported their regulation by microenvironmental signals in both tumor and stromal compartments (7,11). Therefore, they can potentially serve as effectors of successful adaptation to the metastatic microenvironment and subsequent establishment of the metastasis (6).

Most of our knowledge about metastasis comes from the end-point comparison of primary and metastatic tumors (12,13), hence our understanding of metastatic colonization remains limited. *In vitro* models that mimic specific steps only reveal regulators of that step and may or may not continue to be relevant subsequently (14,15). We have previously employed an organotypic 3D culture model of the omentum to study the early steps of metastatic colonization of the omentum (5,7). In the present study, we sought to identify clinically relevant microRNAs that regulate metastasis, by combining

the analysis of matched primary tumors and metastasis from 42 OC patients, with the 3D omentum culture model of early metastatic colonization. This novel approach enabled us to find and target clinically relevant microRNAs that regulate early metastatic colonization and remain essential for advanced metastasis in OC patients. Since OC patients present with extensive peritoneal metastasis with tumors ranging from micro-metastasis to large metastatic lesions, the microRNAs identified would be potential targets for the whole spectrum of metastatic tumors. miR-4454 was identified as a key microRNA downregulated in the OC cells through their interactions with the microenvironmental fibroblasts. Reduced expression of miR-4454 promoted metastasis through the concomitant increase in its targets, SPARC and BAG5, which activated FAK, stabilized mutant p53 and inhibited apoptosis.

Materials and Methods

Reagents

Dulbecco's Modified Eagle Medium (DMEM), minimal essential medium vitamins, minimal essential medium nonessential amino acids, Trypsin and Penicillin–Streptomycin were obtained from Media Tech (Manassas, VA, USA). TaqMan miRNA assay for hsa-miR-4454 was purchased from Applied Biosystems (Foster City, CA, USA). pre-miR-4454 mimic and scrambled or negative control were purchased from Ambion (Thermo Fisher Scientific, Hanover Park, IL). miRCURY LNA anti-miR-4454 and scrambled anti-miR-negative control were from Exiqon (Vedbæk, Denmark). The pre-miR-4454 vector (pSMART hCMV/TURBO GFP miR-4454 Vector) was purchased from Dharmacon (Lafayette, CO, USA), The GFP (Cat# CD511B-1) lentiviral vector, control vectors and the lentivirus packaging kit (Cat# LV500A-1) were purchased from System Biosciences (Mountain View, CA, USA). All the siRNAs used in the study were purchased from Dharmacon (Lafayette, CO, USA) SMARTpool siRNAs: BAG5 siRNA (Cat# J-011960-05-0005); SPARC siRNA (Cat# J-003710-08-0005); Scrambled siRNA (Cat# D-001810-10-20). Thiazolyl blue tetrazolium bromide (MTT reagent, Cat# 298-93-1) was from Acros Organics (Thermo Fisher Scientific, Hanover Park, IL) and 4% paraformaldehyde solution (Cat# NC9245948) was procured from Thermo Fisher Scientific (Hanover Park, IL). Giemsa stain (Cat# GS500) and crystal violet (Cat#C0775) were obtained from Sigma Aldrich (St. Louis, MO).

Cell lines

Human high-grade serous OC cell lines OVCAR3 and OVCAR8 were acquired from Ernst Lengyel (University of Chicago), OVCAR4 was from Joanna Burdette (University of Illinois at Chicago) and Kuramochi from Japanese Collection of Research Bioresources. The cell lines used were genetically validated and tested to be mycoplasma free using respective services from Idexx BioResearch (Columbia, MO). The genetic validation was done using the CellCheck 16 (16 Marker STR Profile and Inter-species Contamination Test) and mycoplasma testing was done using Stat-Myco.

Isolation and culture of primary cells and 3D culture setup for microRNA expression profiling

Human primary mesothelial cells (HPMC) and normal omental fibroblasts (NOF) were isolated from omentum from female donors as described previously (5,7). CAFs were isolated from OC patient metastasis as described previously (11). Primary ovarian cancer cells were isolated from ovarian cancer patient ascites as described by Shepherd *et al* (16) and grown in MCDB/M199 medium with 10ng/ml EGF, 10ng/ml bFGF, 10ug/ml heparin and 1uM cortisol. The 3D omental culture was assembled in 10 cm culture dishes by first seeding (3.6×10^5) normal fibroblasts along with 91 µg of collagen Type 1 (Rat tail, BD Cat#354236) in DMEM. Thereafter, 3.6×10^6 HPMCs were seeded on top of this basement membrane like layer to form a confluent monolayer resembling the mesothelium. The 3D culture was incubated for 24 h to allow the cells to secrete factors to generate the complex microenvironment of the omentum surface layers. GFP-expressing OC cells (1×10^6) were seeded on the 3D culture and allowed to grow for 48 h to investigate the initial events of colonization. Cells were trypsinized and GFP-labeled OC cells were isolated by fluorescence activated cell sorting (FACS) using BD FACS Aria II flow cytometer (BD Biosciences, San Jose, CA). Control cells were grown in regular plastic culture dishes and underwent the same treatment as the 3D culture cells. RNA was isolated from the sorted OC cells using miRNeasy mini kit (Qiagen, Germantown, MD) using the manufacturer's instructions and submitted to NanoString Technologies, Inc (Seattle, WA) for microRNA expression profiling with nCounter miRNA Expression Assay. The high-grade serous OC cells Kuramochi, OVCAR4 and OVCAR8 were used for the microRNA profiling experiments (2 independent experiments/cell).

Population and sample selection for primary tumors and matched metastasis samples for microRNA sequencing

Fresh frozen tumors were collected from stage III-IV high-grade serous epithelial ovarian cancer patients undergoing debulking surgery in the Department of Obstetrics and Gynecology at Mayo Clinic, Rochester as described previously (17). Details of the study populations are provided in Supplementary Table 1. The study was approved by the Mayo Clinic Institutional Review Board.

Tumor microRNA sequencing

Fresh frozen tumor samples were used for microRNA extraction. 1 μg RNA was used to prepare the small RNA libraries using NEBNext Multiplex Small RNA Kit (New England Biolabs; Ipswich, MA) as per the manufacturer's instructions. The cDNA constructs were analyzed with Agilent Bioanalyzer DNA 1000 chip (Santa Clara, CA) and Qubit fluorometry (Invitrogen, Carlsbad, CA). Libraries were sequenced at 12 samples per lane generating ~16 million reads per sample following Illumina's standard protocol using the Illumina HiSeq 2000. The flow cell was sequenced as 50 base single index reads on the Illumina HiSeq 2000, using HiSeq Reagent Kit v3 sequencing reagents and HCS v1.4.8 data collection software. Base-calling was performed using Illumina's RTA v1.12.4.2.

Real-time PCR

RNA was isolated from the cells using miRNeasy Kit (Qiagen Cat# 217004) and used for reverse transcription with Applied Biosystems High Capacity Reverse Transcription Kit (Cat# 4368813) or TaqMan® MicroRNA Reverse Transcription Kit (Cat# 4366597). qRT-PCR was performed for miR-4454 using Taqman miRNA assay (Assay ID 461830_mat) according to the manufacturer's protocol using a Roche LightCycler 96 system with U6 (Assay ID 001973) as endogenous control. Similarly, BAG5 (Assay ID Hs01921361_s1) and SPARC (Assay ID Hs00234160_m1) gene expression qRT-PCR using GAPDH (Assay ID Hs00183740_m1) as a control (5).

Proximal culture

The proximal culture experiments were set up as described previously (18). Kuramochi cells (300K/insert) were seeded in lower surface of a transwell insert with 0.4 μm pores (Corning Cat# 3412), and allowed to incubate for 6 h for cells to attach. The insert was then flipped and placed in a 6-well plate containing growth medium. The human NOFs, CAFs or primary dermal fibroblasts (ATCC, Cat# PCS-201-012) were seeded (150K/insert) on the upper surface of the insert and the cells were allowed to grow for 48

h. At the end point, cells were carefully trypsinized sequentially from each surface without intermixing and collected for RNA isolation and qRT-PCR.

Migration assay

Ovarian cancer cells in serum-free DMEM were seeded in 8 µm pore size cell culture inserts (BD, Falcon) in 3 replicates and allowed to migrate into a lower chamber of the 24-well plate containing DMEM with 10% FBS for 3-6 hours at 37^0C. DMEM with 10% FBS served a chemoattractant in the lower chamber. Cells were fixed in 4% paraformaldehyde at the optimal time points, stained with Giemsa stain for 4 hours, and imaged (5 fields/insert) using the EVOS FL auto microscope (Life Technologies). The number of migrated cells were counted using image-J software (19).

Proliferation assay

Ovarian cancer cells (2000 cells/well) were seeded in 96-well plate in 8 replicates and allowed to grow for 5 days. On the fifth day, MTT (3-(4,5-dimethylthiazol-2-yl)-2,5-diphenyltetrazolium bromide) Assay was conducted to measure proliferation of the ovarian cancer cells by measuring the formazan, an insoluble crystalline product with a deep purple color. The absorbance of the purple color was measured at 560 nm and adjusted for background absorbance at 670 nm using a SynergyH1 plate reader (BioTek) (5).

Colony formation assay

Colony formation assay was performed as described previously (5). Briefly, ovarian cancer cells were seeded in 6-well plates (1000 cells/well) and allowed to form colonies. Once visible colonies were formed, they were fixed with 4% paraformaldehyde and stained with 0.005% crystal violet and were imaged using a Syngene G: Box imaging system and the number of colonies/well were counted using ImageJ software.

Invasion through 3D culture

Cellular invasion through the surface of the omentum was assayed *in vitro* using the 3D omentum culture in 8 µm pore size Fluoroblock transwell inserts in 24 well plates. As described previously (5), the 3D omentum culture was setup in fluoroblock transwell inserts placed in a 24-well plate. GFP-expressing ovarian cancer cells were then seeded on the 3D culture in the transwell insert in serum-free DMEM. DMEM with 10% FBS

served as a chemoattractant in the lower chamber of the 24-well plate. Cells were allowed to invade for 12-16 h, fixed with 4% paraformaldehyde, imaged (5 fields/insert) using EVOS FL Auto (Life Technologies), and counted using ImageJ.

Colony formation on 3D culture

The ability of OC cells to colonize the surface layers of the omentum was assayed by assembling the 3D omentum culture in 6 well plates, as described previously (5). GFP expressing OVCAR8 cells (500 cells/well) were seeded on the 3D omentum culture and allowed to form colonies for 6 days. The fluorescent colonies were imaged using Syngene G:Box imaging system and the colonies were counted.

Mouse xenograft model of OC metastasis

miR-4454 was stably expressed in OVCAR8 cells by infecting them with lentiviral particles containing pre-miR-4454 expression vector (pSMART hCMV/TURBO GFP miR-4454 Vector, Dharmacon). In brief, the plasmid construct was purified (Zymopure plasmid Maxi prep Kit, Cat#D4202) and transfected into HEK293T cells along with the packaging vectors (pPACKH1, Systems Biosciences Cat# LV500A) using FuGene HD (Promega, Cat#E2311) and virus concentrated using PEG-*it* solution (System Biosciences, Cat# LV810A-1). OVCAR8 cells were infected with the lentiviral particles containing miR-4454 construct or empty vector. The xenograft model has been described previously (20) (21). Briefly, 5×10^6 OVCAR8 cells stably expressing lenti-pre-miR-4454, or control vector were injected intraperitoneally (0.5 mL/mouse) into 6-week-old, female, athymic nude mice (10 mice/group). Mice were euthanized 35 days after infection and the peritoneal cavity opened up, the tumors were counted, surgically resected and weighed. Pieces of omental tumors were collected and either flash frozen and stored in -80^0C or fixed in buffered formalin and embedded in paraffin to be used for IHC.

Immunohistochemistry

Immunohistochemical experiments were performed by the Immunohistochemistry core facility of Indiana University School of Medicine using 5 μm thick formalin-fixed deparaffinized sections as previously described (7,21). Xenograft tumor tissue sections were probed with anti-Ki-67 (1:300) (SP6, Thermo Scientific, Waltham, MA, USA) and anti-cleaved caspase-3 (1:100) (Asp175, Cell Signaling, Danvers, MA, USA) antibodies.

RNA-seq for miR-4454 target identification

Total RNA was isolated from Kuramochi and OVCAR4 cells overexpressing miR-4454 or the scrambled negative control as described previously (5) and submitted to the Center for Genomics and Bioinformatics core facility, Indiana University, Bloomington for library preparation and next generation sequencing. The library preparation was done using TruSeq Stranded mRNA HT Sample Prep kit (Illumina cat#RS-122-2103) according to the manufacturer's protocol and 8-neucleotide barcodes were added for multiplexing. The barcoded libraries were cleaned by bead cut with AMPure XP beads (Beckman Coulter, cat#A63882), verified using Qubit3 fluorometer (ThermoFisher Scientific) and 2200 TapeStation bioanalyzer (Agilent Technologies), and then pooled. The pool was sequenced on NextSeq 500 (Illumina) with NextSeq75 High Output v2 kit (Illumina cat#FC-404-2005). Paired end 2x42 bp read sequences were generated. The read sequences were de-multiplexed using bcl2fastq (software v2.20.0.422) (22). Trimmomatic (version 0.36; non-default parameters = ILLUMINACLIP:adapter.fasta:2:20:5 LEADING:3 TRAILING:3 SLIDINGWINDOW:4:15 MINLEN:17) was used to trim reads and to remove adapter sequences and low-quality reads. The trimmed reads were mapped using HiSat2 (version 2.1.0) to the *Homo sapiens* genome HG38 with annotation version Gencode_v27. Reads were sorted and indexed in bam format using SAMtools (version 1.7) (23). Read counts for genes were determined using featureCounts (version 1.5.3) part of the subread package. Differential gene expression was performed in R (version 3.4.1) with DeSeq2 (24,25). Adjusted p-value of <0.05 was used to identify significantly differentially expressed genes with a fold change cut off set at 2-fold. Pathway analysis was performed with Metascape (26) using the genes commonly downregulated in the miR-4454 overexpressing Kuramochi and OVCAR4 cells that had a predicted seed match for miR-4454.

3'UTR Assay

3'UTR reporter clones with BAG5 or SPARC 3'UTR inserted downstream of a secreted gaussia luciferase were purchased from GeneCopoea (Cat# HmiT022868-MT05 and HmiT088625-MT05). They also express secreted alkaline phosphatase driven by a CMV promoter, serving as an internal control. The miR-4454 seed matches on the 3'UTRs were mutated as shown in Supplementary Figure 5A, using Quick Change Lightning mutagenesis kit (Stratagene, La Jolla, CA, USA) according to the manufacturer's

protocol. HEK293T cells were co-transfected with the 3'UTR reporters and pre-miR-4454 or scrambled control oligos using TransIT-X2 (Mirus cat# MIR 6004), the conditioned medium collected, and the secreted gaussia luciferase and alkaline phosphatase assayed using Secrete-Pair Dual Luminescence Assay Kit (GeneCopoea Cat# LF031).

Transient transfection

Ovarian cancer cells were transiently transfected with 30 nM scrambled or control siRNA and pre-miR-4454/anti-miR-4454 using TransIT-X2 (Mirus cat# MIR 6004) according to the manufacturer's protocol. For plasmid transfections, 2-3 µg plasmid was transfected using FuGENE HD (Promega Cat# E2311) as per the manufacturer's protocol. The cells were used for experiments 48 hours after transfection or as indicated (5).

Immunoblotting

Immunoblotting was done as previously described (5). Briefly, proteins were separated by 4-20% gradient SDS-PAGE and transferred to nitrocellulose membrane, probed with BAG5 (Santa Cruz Cat# sc-390832), SPARC (Santa Cruz, Cat# sc-73472 or Haematologic Tech,Cat# AON-5031) Cleaved caspase-3 (Cell Signaling, Cat# 9661), cleaved PARP (Cell Signaling, Cat# 5625), phospho-FAK Tyr397(Cell Signaling, Cat# 3283), FAK (Cell Signaling, Cat# 3285) antibodies. Actin (Sigma Aldrich, Cat# G9295) was probed as a loading control. Horseradish peroxidase-linked anti-rabbit (Cell Signaling, Cat# 7074) or anti-mouse (Cell Signaling, Cat# 7076) IgG secondary antibody was used to probe the membrane bound primary antibodies and detected using clarity western ECL substrate (BioRad, Cat# 170-5061).

Coculture experiments

The human primary cells HPMC (6×10^6), NOF and CAF (1.2×10^6) were seeded in 100 mm dishes, incubated for 18-24 hours. GFP-tagged ovarian cancer cells ($1.5 - 2 \times 10^6$) were overlaid onto the HPMC, NOF and CAF, and allowed to grow for 48 hours to enable interact with primary cells and subsequently used for further experiments to validate the initial events of colonization. Cells were washed, trypsinized and fluorescent cancer cells were isolated by fluorescence activated cell sorting (BD FACS Aria II) and used for RNA isolation (7).

Statistical analysis

Data analysis was done by unpaired, two-tailed Student's t-test assuming equal variance of the test and the control populations.

Study approval: The study was approved by the Mayo Clinic Institutional Review Board, Institutional Regulatory Board of Indiana University and St. Vincent's. The mice studies were approved by the Institutional Animal Care and Use Committee of Indiana University, Bloomington.

Results

Identification of MicroRNAs essential for early and advanced OC metastasis

We profiled the microRNA expression changes in matched primary and metastatic tumors from 42 OC patients (Figure 1A; Supplementary Table 1) using next generation microRNA-seq. However, such end-point analysis does not reveal the microRNAs that are involved in the early steps of metastatic colonization. Therefore, using an organotypic 3D culture model of the omentum (Figure 1B) (5) and a panel of 3 high-grade serous OC (HGSOC) cell lines (Kuramochi, OVCAR4 and OVCAR8), we profiled the microRNA expression changes in OC cells occurring during early metastatic colonization. To identify those microRNAs that drive these initial steps and also continue to be essential in the fully formed metastatic tumor, we considered the microRNAs that are commonly deregulated in both OC patient tumors and the 3D omental culture model (Figure 1A). Since global microRNA downregulation is common in OC (27), we focused on the downregulated microRNAs. 26 microRNAs were decreased in the patient metastasis to omentum or bowels as well as in at least 2 HGSOC cells on 3D omental culture (Supplementary Table 2). These microRNAs were analyzed for the microRNA-target interaction networks (Figure 1C) using miRNet (28). Similarly, using miRSystem (29), the pathways that can be potentially regulated by these common microRNAs were identified as developmental, MAP kinase, regulation of actin cytoskeleton, axon guidance, ERBB1 signaling and focal adhesions (Supplementary Figure 1A). All of these can potentially play a role in metastasis. Only miR-4454 was significantly downregulated across all the 3 OC cell lines and OC patient metastases (Supplementary Table 2). The sequencing results were validated by qRT-PCR for miR-4454 in a set of OC patient primary and omental metastasis (Figure 1D *Top*) as well as in Kuramochi, OVCAR4 and OVCAR8 cells seeded on the 3D omental culture (Figure 1D *Bottom*). To further confirm the results, we isolated OC cells from ascites of 2 patients and seeded them on the 3D

omental culture. miR-4454 expression was decreased significantly in both the ascites derived OC cells seeded on the 3D culture (Figure 1E). Endogenous expression of miR-4454 was lower in OC cells compared to normal cells (Supplementary Figure 1B). A time-course experiment ranging from 12 to 72 hours indicated that the maximal downregulation of miR-4454 occurred within 48 hours (Supplementary Figure 1C). An analysis of miR-4454 expression in the patient cohort showed that decreased miR-4454 expression in metastasis correlated with poor outcome (Figure 1F). Therefore, miR-4454 was selected for further studies.

Functional role of miR-4454 in metastasis

To test if miR-4454 had a relevant functional role in metastasis, a panel of HGSOC cells – Kuramochi, OVCAR3, OVCAR4 and OVCAR8 – were transiently transfected with pre-miR-4454 (Supplementary Figure 2A) and the effect of overexpression was tested on their ability to migrate, proliferate and form colonies. Overexpression of miR-4454 reduced migration, proliferation and colony formation in all the 4 HGSOC cells compared to those transfected with the scrambled negative control oligos (Figure 2A and Supplementary Figure 2 B and C). To study the effect of miR-4454 inhibition, the HGSOC cells were transfected with anti-miR-4454 or control oligos (Supplementary Figure 2D). Inhibition of miR-4454 resulted in an increase in migration, proliferation and colony formation (Figure 2B and Supplementary Figure 2 E and F). This suggested that the downregulation of miR-4454 during early steps of metastatic colonization equips them with abilities to colonize the metastatic site. The effect of miR-4454 on the capacity of the OC cells to invade through the surface layers of the omentum, which is an essential initial step for successful metastatic colonization, was studied next. The omental 3D culture was assembled in fluoroblock transwell inserts and fluorescent OC cells were seeded and allowed to invade through it and the number of invaded OC cells on the bottom surface of the insert was quantified (Figure 2C) (5). Overexpression of miR-4454 resulted in decreased invasion through the surface layers of the omentum, while inhibition of miR-4454 had the opposite effect (Figure 2 D). Furthermore, we also mimicked the ability of the cancer cells to colonize the omentum by seeding GFP expressing cells on the 3D omentum culture and quantifying the fluorescent colonies formed. Overexpression of miR-4454 resulted in decreased OVCAR8 colonies on the 3D omentum culture, while inhibition had the opposite effect (Figure 2E). This clearly

indicated that miR-4454 downregulation played an important role in driving the initial colonization of the omentum.

miR-4454 overexpression inhibits metastasis *in vivo*

We next tested the sustained role of miR-4454 during progression of metastasis *in vivo*. OVCAR8 is one of the most effective HGSOC cells for xenograft experiments (20). We stably overexpressed miR-4454 in OVCAR8 cells using a lentiviral expression system (Supplementary Figure 3A) and confirmed its effect on migration, proliferation and colony formation (Supplementary Figure 3B). These cells were then injected intraperitoneally in female nude mice to assess their ability to form peritoneal metastasis as compared to the vector controls (20). Mice were euthanized 35 days after injection, the tumors were counted, surgically isolated and weighed. Stable overexpression of miR-4454 resulted in a significant decrease in the number of metastasis (Figure 3A) and total tumor weight (Figure 3B). Representative images of tumor bearing mice are shown in Figure 3C. Portions of the omental tumors were used to confirm the stable overexpression of miR-4454 in these tumors by qRT-PCR (Figure 3D). There was a marked increase in apoptosis in the tumors overexpressing miR-4454 as indicated by the increased cleaved caspase 3 observed in these tumors (Figure 3E). On the contrary, the miR-4454 tumors had decreased proliferation as evidenced by the reduced expression of Ki-67 (Figure 3F). This confirmed the importance of miR-4454 for metastasis *in vivo*.

Paracrine signals from microenvironmental fibroblasts downregulate miR-4454

To identify the cellular component of the omental microenvironment that could induce miR-4454 downregulation, the OC cells were cocultured with mesothelial cells and normal omental fibroblasts (NOFs). A significant miR-4454 downregulation was observed upon coculture with NOFs, while mesothelial cells had the opposite effect (Figure 4A). Since miR-4454 is downregulated in patient metastasis, and cancer associated fibroblasts (CAFs) constitute a significant percentage of the tumor microenvironment (11), the OC cells were cocultured with CAFs and that decreased miR-4454 (Figure 4A). Such heterotypic cocultures can involve paracrine or juxtacrine signaling. Treatment of OC cells with conditioned medium from omental fibroblasts or CAFs did not downregulate miR-4454 (Figure 4B). This could indicate that there is no secreted factor involved or that the continuous high localized concentrations of factors

experienced by the OC cells and fibroblasts, when in close proximity, is essential for triggering miR-4454 downregulation. Proximal culture (18) of OC cells and fibroblasts/CAFs, separated by a 10 μm thick membrane with 0.4 μm pores that allow constant exchange of paracrine factors at localized physiological concentrations (Figure 4C), decreased miR-4454 (Figure 4D). This indicates that the continuous localized high concentrations of paracrine factors maintained by the proximal culture is essential for miR-4454 downregulation. Therefore, the initial paracrine interactions of the metastasizing OC cells with the NOFs in the basement membrane of the omentum resulted in the downregulation of miR-4454. As the metastatic tumor progressed, the CAFs in the tumor microenvironment continued to provide the paracrine signaling necessary to sustain miR-4454 downregulation. Proximal culture with human dermal fibroblasts did not have any effect on miR-4454 (Figure 4D).

Identification of miR-4454 targets

Since microRNAs act pleiotropically by the translational inhibition of multiple target genes, it was crucial to identify the key target genes whose expression was increased as a result of miR-4454 downregulation and how they mediated the functional effects of miR-4454. miR-4454 was overexpressed in Kuramochi and OVCAR4 cells followed by RNA-seq. 2012 and 1868 genes were significantly downregulated in Kuramochi and OVCAR4 cells respectively and 811 genes were common to both (Figure 5A and Supplementary Figure 4 A and B). Using microRNA target prediction software TargetScan, miRDB and TargetMiner, the 811 common genes were analyzed for predicted miR-4454 seed matches. 68 genes were predicted to be a miR-4454 target by at least one software (Figure 5B). A pathway analysis of these genes using Metascape (26) revealed 6 key pathways in which these targets are involved (Supplementary Figure 4C and D). A literature search was done to identify the cancer/metastasis relevant genes among these potential targets (Supplementary Table 3). Based on this, we selected SPARC, BAG5, and SRY-box 4 (SOX4) for testing as functional effectors of miR-4454. SPARC, a cysteine-rich acidic matrix-associated protein, has been reported to promote metastasis in head and neck squamous cell carcinoma (30). It is associated with higher OC disease stage (31) and helps in deposition of TGFβ1 on ECM (32). BAG5, an antiapoptotic protein, inhibits ER-stress induced apoptosis in prostate cancer (33). It also supports mutant p53 accumulation and gain of function, promoting proliferation, migration and chemoresistance (34). SOX4 is a transcription factor that acts as an

oncogene in OC (35). qRT-PCR was done for these 3 genes to validate the sequencing results. SPARC and BAG5 were significantly downregulated upon miR-4454 overexpression in both Kuramochi and OVCAR4 cells (Figure 5C). The baseline expression of SOX4 was too low in both the cells. Therefore, we focused on SPARC and BAG5 as candidates for mediating the effects of miR-4454 on OC metastasis. To confirm if they are direct targets of miR-4454, we performed a 3'UTR reporter assay using wild type (WT) or miR-4454 seed match mutated (Mut) BAG5 or SPARC 3'UTRs (Supplementary Figure 5A) linked to Gaussia luciferase. These constructs also express secreted alkaline phosphatase for transfection normalization. They were co-transfected with pre-miR-4454 or scrambled controls in HEK293T cells and the secreted Gaussia luciferase activity was assayed and normalized to alkaline phosphatase using secreted pair dual luminescence assay kit (GeneCopoeia). While the WT 3'UTRs of BAG5 and SPARC reduced luciferase activity in presence of miR-4454, mutating the seed match reverted them back to that overserved in scrambled controls (Figure 5D).

BAG5 and SPARC are functional effectors of miR-4454

To serve as downstream effectors of miR-4454, BAG5 and SPARC should be able to affect OC cell migration, proliferation and clonogenic growth. Silencing BAG5 or SPARC in Kuramochi, OVCAR4 and OVCAR8 cells resulted in a decrease in migration, proliferation and colony formation (Figure 5 E and F and Supplementary Figure 5 B-E). To confirm if BAG5 and SPARC are direct downstream effectors of miR-4454, functional rescue experiments were done. miR-4454 was inhibited and simultaneously BAG5 or SPARC were silenced in Kuramochi cells. As expected, inhibition of miR-4454 increased the ability of cells to migrate, proliferate and form colonies while silencing BAG5 or SPARC had an inhibitory effect (Figure 6 A-C). However, simultaneous inhibition of miR-4454 along with silencing BAG5 or SPARC reverted the migration and proliferation back to the scrambled negative control levels (Figure 6 A and B). The rescue was partial in the case of colony formation assay (Figure 6C). Therefore, silencing BAG5 or SPARC could rescue the respective functions of OC cells caused by miR-4454, confirming them as downstream effectors of the microRNA. KM-plotter analysis (36) revealed that increased expression of BAG5 or SPARC resulted in worse progression free survival with a hazard ratio of 1.37 and 1.43 respectively (Figure 6D).

Mechanism of regulation of OC metastasis by miR-4454 through BAG5 and SPARC

BAG5 is an antiapoptotic protein, which protects from ER-stress (33) and helps mutant p53 gain of function by promoting its accumulation (34). SPARC is a secreted protein that can mediate interactions with the ECM and growth factors trapped therein (37). Therefore, to understand the mechanism of action of miR-4454 though its targets BAG5 and SPARC, we studied the effects of miR-4454 overexpression on apoptosis and cellular signaling in OC cells. miR-4454 overexpression and the concomitant decreased expression of BAG5 resulted in increased apoptosis, evidenced by increased cleaved PARP and caspase 3, and decrease in the mutant p53 levels (OVCAR3: R248Q; OVCAR4: L130V) (Figure 7A, left). The silencing of BAG5 resulted in a similar increased cleavage of PARP and caspase 3 (Figure 7A, right). It also decreased the mutant p53 levels indicating its role in mutant p53 stabilization and gain of function. miR-4454 overexpression was coupled to a decrease in SPARC, which reduced phosphorylation of FAK at the auto phosphorylation site (Tyr397) (Figure 7B, left). FAK phosphorylation at Tyr397 was also inhibited in cells transfected with SPARC siRNA (Figure 7B, right). Taken together, the data indicate that miR-4454 downregulation predominantly results in increased growth and invasion through the activation of FAK by the increased expression of SPARC. At the same time, BAG5 promoted mutant p53 gain of function by stabilizing it and inhibited apoptosis. Together they effectively equip the OC cells for metastatic colonization (summarized in Figure 7C).

Discussion

Increasing interest in the tumor microenvironment has resulted in a better understanding of its importance in tumor progression (3,38,39). We are starting to learn more about the metastatic microenvironment and its role in successful metastatic colonization (5,7,40). This has been facilitated by the advent of various 3D culture models that replicate the OC metastatic microenvironment in tissue culture (14). While these models have provided key insights into the reciprocal interactions between the OC cells and the metastatic microenvironment, our knowledge of the master regulators of this process remains limited. micoRNAs can act as master regulators of multiple processes and have been implicated in many steps of cancer progression, including metastasis (6,8). Moreover, using 3D culture models, we have demonstrated that microRNA expression in both OC cells and stromal cells can get altered as a result of the reciprocal interactions

between OC cells and the microenvironment (7,11). These microRNAs act as master regulators driving metastatic colonization in case of OC cells or reprogram normal omental fibroblasts into CAFs.

The information obtained employing the 3D culture models is still limited to the early steps of colonization. Therefore, the question remains if these microRNAs are relevant in the fully formed metastatic tumors. Since therapeutic interventions will treat such fully formed metastatic tumors, it would be important to study those microRNAs that are essential for early colonization and remain important for the advanced metastasis. Towards this end, we have profiled the microRNA expression of matched primary and metastatic tumors from 42 OC patients. Analysis of microRNA changes in end point metastasis compared to primary tumors have been reported for OC previously, but do not involve such large number of samples (9). Importantly, these studies lack information about those microRNAs that are vital for early metastatic colonization – the rate limiting step of metastasis. Therefore, our comprehensive approach to combine the microRNA profiling data from the 3D omental model mimicking early metastasis with that obtained from paired primary and metastatic tumors identifies those clinically relevant microRNAs that are altered by interactions of OC cells with the microenvironment during early colonization and remain essential in the fully developed metastatic tumors. This is the first report employing this novel and comprehensive approach to identify clinically relevant master regulators of OC metastasis.

This approach helped identify miR-4454 as a metastasis suppressor. It is located on chromosome 4 and till date, very little is known about its function in cancer (10,41). miR-4454 overexpression has also been reported to cause degeneration of chondrocytes (42). It has been reported as one of the microRNAs that are upregulated in HeLa cells upon treatment with TNFα (43). In an analysis of microRNAs expression in FFPE tumors and body fluids of 16 bladder cancer patients, miR-4454 was detected in the tumors, urine and white blood cells (44). It was among the 25 microRNAs found to be differentially expressed in the plasma of 6 metastatic melanoma patients before and after surgery to remove the tumors (10). miR-4454 was also found in all subtypes of EVs secreted by the human colon carcinoma cell line LIM1863 (45). Of note, our study indicated that miR-4454 was downregulated in metastasis as compared to primary tumor in OC patients. This downregulation was induced by the cross-talk with omental

fibroblasts. A potential mechanism of downregulation could be efflux through secreted EVs. Like many other microRNAs, miR-4454 downregulation had pleotropic effects on cellular functions through its targets. Most importantly, its downregulation was essential for the initial adaptation of the OC cells to the metastatic microenvironment as well as the subsequent tumor growth and ultimately important for the large metastatic tumor as well. Therefore, miR-4454 is an optimal target for treating OC metastasis where the metastatic tumors can range from micro-metastasis to large tumors (3). We also established that it plays a very important part in the initial invasion of the OC cells through the mesothelium and the basement membrane of the omentum. This is one of the most important initial steps involved in the process of metastatic colonization (46,47). The effect of stable overexpression of miR-4454 on inhibiting metastasis in OC mouse xenografts indicated its importance in the later stages of metastatic tumor development *in vivo*.

Using RNA-seq we identified SPARC and BAG5 as key targets of miR-4454. SPARC is a secreted glycoprotein with pleotropic functions that has been implicated in pathogenic conditions like cancer progression, obesity and diabetes (48,49). It can play a role in mediating the interactions between cancer cells and the extracellular microenvironment and regulates adhesion, migration and proliferation (50). Increased expression of SPARC resulted in an increase in the deposition of TGFβ1 in the mesothelial ECM (32). The tumor stroma is a major contributor of SPARC and contributes towards poor outcome (51). However, it has also been reported to act as a tumor suppressor by inhibiting OC interactions with adipocytes and certain ECM proteins (52,53). Although SPARC is associated with poor prognosis in pancreatic cancer (48), there have been conflicting reports on SPARC having oncogenic or tumor suppressor functions (48). Our analysis of publicly available databases revealed that it significantly correlated with poor OC patient prognosis. This agrees with the findings of Chen et al., who reported that increased SPARC expression was associated with higher grade and stage and poorer prognosis in ovarian cancer (31). They observed higher expression levels of SPARC in more invasive OC. The clinical relevance of SPARC in OC metastasis is further highlighted by the effective use of SPARC targeting imaging nanoprobes to detect OC micro-metastasis for surgical guidance (54). SPARC has been reported to promote migration through activation of stress fibers and focal adhesions, which in turn activated FAK (55). Increased expression of SPARC was detected at the tumor–stromal interface

of the invading ovarian tumors (56). Our data also supports this mechanism as both miR-4454 overexpression and SPARC silencing reduced FAK phosphorylation at Tyr397 – the autophosphorylation site. SPARC has also been reported to activate AKT, TGFβ and MAP kinase pathways (48,57). However, we were not able to confirm these effects in our models (data not shown). BAG5, an antiapoptotic protein, is a unique member of the Bcl-2-associated athanogene family proteins, containing 5 BAG domains (58). It interacts with the molecular chaperone GRP78/BiP to inhibit apoptosis and increase stress tolerance in prostate cancer (33). Our data similarly indicates that BAG5 mediates the antiapoptotic effects of miR-4454 downregulation during metastasis. Overcoming apoptosis is key to surviving in the new metastatic microenvironment encountered by the cancer cells (59). Therefore, BAG5 equips OC cells with this important ability and helps them establish the metastatic tumor. Interestingly, binding of BAG5 to mutant p53 can lead to its accumulation and promotion of its gain of function activity including cellular migration, proliferation and tumor growth (34). Our data supports this function of BAG5. Since almost all HGSOC tumors have mutations in p53, this could potentially explain the inhibitory effects of BAG5 silencing on migration, proliferation and colony formation observed by us.

A recent comprehensive study on deconstructing omental metastasis of OC patients also revealed that both SPARC and BAG5 are highly expressed in the metastatic tumors (60). Silencing SPARC and BAG5 could functionally rescue the effects of miR-4454 inhibition on OC cells, establishing them as downstream effectors. They enable OC cells to invade, proliferate and overcome apoptosis as they try to establish the metastatic tumor in the new microenvironment. Interestingly, normal omental fibroblasts, one of the first microenvironmental components encountered by the OC cells at the metastatic site, induce the downregulation of miR-4454. This suggests that these omental fibroblasts are unique and can potentially serve as the optimal seed for the establishment of metastatic tumors and could be a contributing factor towards the ability OC to successfully metastasize within the peritoneum. As the metastasis progresses, the normal fibroblasts are replaced by CAFs in the tumor microenvironment and they take over the job of continuing to provide the paracrine signals essential to maintain the downregulation of miR-4454. Therefore, targeting miR-4454 could possibly be an effective approach to treat micro-metastasis as well as advanced metastasis. The effect of stable overexpression of miR-4454 on metastasis in xenografts supports the translational

potential of such an approach. Future directions include research towards determining the mechanism of cross-talk between the fibroblasts and OC cells and exploring the potential of preclinical targeting of miR-4454 with precursor constructs as an effective therapy for OC metastasis.

Author Contributions

SD and TP performed the experiments and data analysis. TG, DWV, FM, AM and VS were involved in planning, sample collection and execution of the microRNA profiling of OC patient tumors. AM, SD and VS also helped with manuscript preparation. KA helped with the 3D omental culture model. AKM was involved in conception, design, supervision, analysis and interpretation of data and manuscript preparation.

Acknowledgments

We are deeply indebted to the patients for their generosity and thankful to Dr. Xiongbin Lu for critically reviewing the manuscript. We also acknowledge the help of the 'Center for Genomics and Bioinformatics' and 'Flow Cytometry Core Facility' at IU Bloomington as well as the 'Immunohistochemistry Core' of IUSM.

This research was supported by DoD OCRP Ovarian Cancer Academy Award (W81XWH-15-0253), Colleen's Dream Foundation, CTSI core pilot and Ralph W. and Grace M. Showalter Research awards. The tumor collection and miRNAseq was supported in part by the grants from the National Institutes of Health (P50CA136393), Andersen Foundation grant (AM), the Department of Experimental Pathology and Laboratory Medicine, and Mayo Clinic (VS).

References

1. Torre LA, Trabert B, DeSantis CE. Ovarian cancer statistics, 2018. **2018**;68(4):284-96 doi 10.3322/caac.21456.
2. Siegel RL, Miller KD, Jemal A. Cancer statistics, 2018. CA: a cancer journal for clinicians **2018**;68(1):7-30 doi 10.3322/caac.21442.
3. Bowtell DD, Bohm S, Ahmed AA, Aspuria PJ, Bast RC, Jr., Beral V, *et al.* Rethinking ovarian cancer II: reducing mortality from high-grade serous ovarian cancer. Nature reviews Cancer **2015**;15(11):668-79 doi 10.1038/nrc4019.

4. Chambers AF, Groom AC, MacDonald IC. Dissemination and growth of cancer cells in metastatic sites. Nature reviews Cancer **2002**;2(8):563-72 doi 10.1038/nrc865.
5. Tomar S, Plotnik JP, Haley J, Scantland J, Dasari S, Sheikh Z*, et al.* ETS1 induction by the microenvironment promotes ovarian cancer metastasis through focal adhesion kinase. Cancer letters **2018**;414:190-204 doi 10.1016/j.canlet.2017.11.012.
6. Pencheva N, Tavazoie SF. Control of metastatic progression by microRNA regulatory networks. Nature cell biology **2013**;15(6):546-54 doi 10.1038/ncb2769.
7. Mitra AK, Chiang CY, Tiwari P, Tomar S, Watters KM, Peter ME*, et al.* Microenvironment-induced downregulation of miR-193b drives ovarian cancer metastasis. Oncogene **2015**;34(48):5923-32 doi 10.1038/onc.2015.43.
8. Kohlhapp FJ, Mitra AK, Lengyel E, Peter ME. MicroRNAs as mediators and communicators between cancer cells and the tumor microenvironment. Oncogene **2015**;34(48):5857-68 doi 10.1038/onc.2015.89.
9. Vang S, Wu HT, Fischer A, Miller DH, MacLaughlan S, Douglass E*, et al.* Identification of ovarian cancer metastatic miRNAs. PloS one **2013**;8(3):e58226 doi 10.1371/journal.pone.0058226.
10. Latchana N, DiVincenzo MJ, Regan K, Abrams Z, Zhang X, Jacob NK*, et al.* Alterations in patient plasma microRNA expression profiles following resection of metastatic melanoma. **2018**;118(3):501-9 doi 10.1002/jso.25163.
11. Mitra AK, Zillhardt M, Hua Y, Tiwari P, Murmann AE, Peter ME*, et al.* MicroRNAs Reprogram Normal Fibroblasts into Cancer Associated Fibroblasts in Ovarian Cancer. Cancer discovery **2012**;2(12):1100-8 doi 10.1158/2159-8290.CD-12-0206.
12. Lee JY, Yoon JK, Kim B, Kim S, Kim MA, Lim H*, et al.* Tumor evolution and intratumor heterogeneity of an epithelial ovarian cancer investigated using next-generation sequencing. BMC cancer **2015**;15:85 doi 10.1186/s12885-015-1077-4.
13. Lancaster JM, Dressman HK, Clarke JP, Sayer RA, Martino MA, Cragun JM*, et al.* Identification of genes associated with ovarian cancer metastasis using microarray expression analysis. International journal of gynecological cancer : official journal of the International Gynecological Cancer Society **2006**;16(5):1733-45 doi 10.1111/j.1525-1438.2006.00660.x.
14. Watters KM, Bajwa P, Kenny HA. Organotypic 3D Models of the Ovarian Cancer Tumor Microenvironment. **2018**;10(8) doi 10.3390/cancers10080265.
15. Iwanicki MP, Davidowitz RA, Ng MR, Besser A, Muranen T, Merritt M*, et al.* Ovarian cancer spheroids use myosin-generated force to clear the mesothelium. Cancer discovery **2011**;1(2):144-57 doi 10.1158/2159-8274.cd-11-0010.

16. Shepherd TG, Theriault BL, Campbell EJ, Nachtigal MW. Primary culture of ovarian surface epithelial cells and ascites-derived ovarian cancer cells from patients. Nature protocols **2006**;1(6):2643-9 doi 10.1038/nprot.2006.328.
17. Mariani A, Wang C, Oberg AL, Riska SM, Torres M, Kumka J*, et al.* Genes associated with bowel metastases in ovarian cancer. Gynecologic oncology **2019**;154(3):495-504 doi 10.1016/j.ygyno.2019.06.010.
18. Dasari S, Pandhiri T, Haley J, Lenz D, Mitra AK. A Proximal Culture Method to Study Paracrine Signaling Between Cells. Journal of visualized experiments : JoVE **2018**(138) doi 10.3791/58144.
19. Haley J, Tomar S, Pulliam N, Xiong S, Perkins SM, Karpf AR*, et al.* Functional characterization of a panel of high-grade serous ovarian cancer cell lines as representative experimental models of the disease. Oncotarget **2016**;7(22):32810-20 doi 10.18632/oncotarget.9053.
20. Mitra AK, Davis DA, Tomar S, Roy L, Gurler H, Xie J*, et al.* In vivo tumor growth of high-grade serous ovarian cancer cell lines. Gynecologic oncology **2015**;138(2):372-7 doi 10.1016/j.ygyno.2015.05.040.
21. Mitra AK, Sawada K, Tiwari P, Mui K, Gwin K, Lengyel E. Ligand-independent activation of c-Met by fibronectin and alpha(5)beta(1)-integrin regulates ovarian cancer invasion and metastasis. Oncogene **2011**;30(13):1566-76 doi 10.1038/onc.2010.532.
22. Bolger AM, Lohse M, Usadel B. Trimmomatic: a flexible trimmer for Illumina sequence data. Bioinformatics (Oxford, England) **2014**;30(15):2114-20 doi 10.1093/bioinformatics/btu170.
23. Li H, Handsaker B, Wysoker A, Fennell T, Ruan J, Homer N*, et al.* The Sequence Alignment/Map format and SAMtools. Bioinformatics (Oxford, England) **2009**;25(16):2078-9 doi 10.1093/bioinformatics/btp352.
24. Liao Y, Smyth GK, Shi W. featureCounts: an efficient general purpose program for assigning sequence reads to genomic features. Bioinformatics (Oxford, England) **2014**;30(7):923-30 doi 10.1093/bioinformatics/btt656.
25. Love MI, Huber W, Anders S. Moderated estimation of fold change and dispersion for RNA-seq data with DESeq2. Genome biology **2014**;15(12):550 doi 10.1186/s13059-014-0550-8.
26. Tripathi S, Pohl MO, Zhou Y, Rodriguez-Frandsen A, Wang G, Stein DA*, et al.* Meta- and Orthogonal Integration of Influenza "OMICs" Data Defines a Role for UBR4 in Virus Budding. Cell host & microbe **2015**;18(6):723-35 doi 10.1016/j.chom.2015.11.002.
27. Zhang L, Volinia S, Bonome T, Calin GA, Greshock J, Yang N*, et al.* Genomic and epigenetic alterations deregulate microRNA expression in human epithelial ovarian cancer. Proceedings of the National Academy of Sciences of the United States of America **2008**;105(19):7004-9 doi 10.1073/pnas.0801615105.
28. Fan Y, Xia J. miRNet-Functional Analysis and Visual Exploration of miRNA-Target Interactions in a Network Context. Methods in molecular biology (Clifton, NJ) **2018**;1819:215-33 doi 10.1007/978-1-4939-8618-7_10.
29. Lu T-P, Lee C-Y, Tsai M-H, Chiu Y-C, Hsiao CK, Lai L-C*, et al.* miRSystem: an integrated system for characterizing enriched functions and pathways of

microRNA targets. PloS one **2012**;7(8):e42390-e doi 10.1371/journal.pone.0042390.

30. Benaich N, Woodhouse S, Goldie SJ, Mishra A, Quist SR, Watt FM. Rewiring of an epithelial differentiation factor, miR-203, to inhibit human squamous cell carcinoma metastasis. Cell reports **2014**;9(1):104-17 doi 10.1016/j.celrep.2014.08.062.
31. Chen J, Wang M, Xi B, Xue J, He D, Zhang J, *et al.* SPARC is a key regulator of proliferation, apoptosis and invasion in human ovarian cancer. PloS one **2012**;7(8):e42413 doi 10.1371/journal.pone.0042413.
32. Tumbarello DA, Andrews MR, Brenton JD. SPARC Regulates Transforming Growth Factor Beta Induced (TGFBI) Extracellular Matrix Deposition and Paclitaxel Response in Ovarian Cancer Cells. PloS one **2016**;11(9):e0162698 doi 10.1371/journal.pone.0162698.
33. Bruchmann A, Roller C, Walther TV, Schafer G, Lehmusvaara S, Visakorpi T, *et al.* Bcl-2 associated athanogene 5 (Bag5) is overexpressed in prostate cancer and inhibits ER-stress induced apoptosis. BMC cancer **2013**;13:96 doi 10.1186/1471-2407-13-96.
34. Yue X, Zhao Y, Huang G, Li J, Zhu J, Feng Z, *et al.* A novel mutant p53 binding partner BAG5 stabilizes mutant p53 and promotes mutant p53 GOFs in tumorigenesis. Cell discovery **2016**;2:16039 doi 10.1038/celldisc.2016.39.
35. Yeh YM, Chuang CM, Chao KC, Wang LH. MicroRNA-138 suppresses ovarian cancer cell invasion and metastasis by targeting SOX4 and HIF-1alpha. International journal of cancer Journal international du cancer **2013**;133(4):867-78 doi 10.1002/ijc.28086.
36. Lanczky A, Nagy A, Bottai G, Munkacsy G, Szabo A, Santarpia L, *et al.* miRpower: a web-tool to validate survival-associated miRNAs utilizing expression data from 2178 breast cancer patients. Breast cancer research and treatment **2016**;160(3):439-46 doi 10.1007/s10549-016-4013-7.
37. Podhajcer OL, Benedetti LG, Girotti MR, Prada F, Salvatierra E, Llera AS. The role of the matricellular protein SPARC in the dynamic interaction between the tumor and the host. Cancer metastasis reviews **2008**;27(4):691-705 doi 10.1007/s10555-008-9146-7.
38. Hanahan D, Coussens LM. Accessories to the crime: functions of cells recruited to the tumor microenvironment. Cancer cell **2012**;21(3):309-22 doi 10.1016/j.ccr.2012.02.022.
39. Lee W, Ko SY, Mohamed MS, Kenny HA, Lengyel E, Naora H. Neutrophils facilitate ovarian cancer premetastatic niche formation in the omentum. **2019**;216(1):176-94 doi 10.1084/jem.20181170.
40. Peinado H, Zhang H, Matei IR, Costa-Silva B, Hoshino A, Rodrigues G, *et al.* Pre-metastatic niches: organ-specific homes for metastases. Nature reviews Cancer **2017**;17(5):302-17 doi 10.1038/nrc.2017.6.
41. McCann MJ, Rotjanapun K, Hesketh JE, Roy NC. Expression profiling indicating low selenium-sensitive microRNA levels linked to cell cycle and cell stress response pathways in the CaCo-2 cell line. The British journal of nutrition **2017**;117(9):1212-21 doi 10.1017/s0007114517001143.

42. Nakamura A, Rampersaud YR. Identification of microRNA-181a-5p and microRNA-4454 as mediators of facet cartilage degeneration. **2016**;1(12):e86820.
43. Zhou F, Wang W, Xing Y, Wang T, Xu X, Wang J. NF-kappaB target microRNAs and their target genes in TNFalpha-stimulated HeLa cells. Biochimica et biophysica acta **2014**;1839(4):344-54 doi 10.1016/j.bbagrm.2014.01.006.
44. Armstrong DA, Green BB, Seigne JD, Schned AR, Marsit CJ. MicroRNA molecular profiling from matched tumor and bio-fluids in bladder cancer. Molecular cancer **2015**;14:194 doi 10.1186/s12943-015-0466-2.
45. Ji H, Chen M, Greening DW, He W, Rai A, Zhang W, *et al.* Deep sequencing of RNA from three different extracellular vesicle (EV) subtypes released from the human LIM1863 colon cancer cell line uncovers distinct miRNA-enrichment signatures. PloS one **2014**;9(10):e110314 doi 10.1371/journal.pone.0110314.
46. Tan DS, Agarwal R, Kaye SB. Mechanisms of transcoelomic metastasis in ovarian cancer. The Lancet Oncology **2006**;7(11):925-34 doi 10.1016/s1470-2045(06)70939-1.
47. Barbolina MV. Molecular Mechanisms Regulating Organ-Specific Metastases in Epithelial Ovarian Carcinoma. Cancers **2018**;10(11) doi 10.3390/cancers10110444.
48. Vaz J, Ansari D, Sasor A, Andersson R. SPARC: A Potential Prognostic and Therapeutic Target in Pancreatic Cancer. Pancreas **2015**;44(7):1024-35 doi 10.1097/mpa.0000000000000409.
49. Kos K, Wilding JP. SPARC: a key player in the pathologies associated with obesity and diabetes. Nature reviews Endocrinology **2010**;6(4):225-35 doi 10.1038/nrendo.2010.18.
50. Wong SL, Sukkar MB. The SPARC protein: an overview of its role in lung cancer and pulmonary fibrosis and its potential role in chronic airways disease. British journal of pharmacology **2017**;174(1):3-14 doi 10.1111/bph.13653.
51. Busuttil RA, George J, Tothill RW, Ioculano K, Kowalczyk A, Mitchell C, *et al.* A signature predicting poor prognosis in gastric and ovarian cancer represents a coordinated macrophage and stromal response. Clinical cancer research : an official journal of the American Association for Cancer Research **2014**;20(10):2761-72 doi 10.1158/1078-0432.Ccr-13-3049.
52. John B, Naczki C, Patel C, Ghoneum A, Qasem S, Salih Z, *et al.* Regulation of the bi-directional cross-talk between ovarian cancer cells and adipocytes by SPARC. Oncogene **2019**;38(22):4366-83 doi 10.1038/s41388-019-0728-3.
53. Said N, Najwer I, Motamed K. Secreted protein acidic and rich in cysteine (SPARC) inhibits integrin-mediated adhesion and growth factor-dependent survival signaling in ovarian cancer. The American journal of pathology **2007**;170(3):1054-63 doi 10.2353/ajpath.2007.060903.
54. Ghosh D, Bagley AF, Na YJ, Birrer MJ, Bhatia SN, Belcher AM. Deep, noninvasive imaging and surgical guidance of submillimeter tumors using targeted M13-stabilized single-walled carbon nanotubes. Proceedings of the

National Academy of Sciences of the United States of America **2014**;111(38):13948-53 doi 10.1073/pnas.1400821111.

55. Dejeans N, Pluquet O, Lhomond S, Grise F, Bouchecareilh M, Juin A*, et al.* Autocrine control of glioma cells adhesion and migration through IRE1alpha-mediated cleavage of SPARC mRNA. Journal of cell science **2012**;125(Pt 18):4278-87 doi 10.1242/jcs.099291.
56. Brown TJ, Shaw PA, Karp X, Huynh MH, Begley H, Ringuette MJ. Activation of SPARC expression in reactive stroma associated with human epithelial ovarian cancer. Gynecologic oncology **1999**;75(1):25-33 doi 10.1006/gyno.1999.5552.
57. Francki A, McClure TD, Brekken RA, Motamed K, Murri C, Wang T*, et al.* SPARC regulates TGF-beta1-dependent signaling in primary glomerular mesangial cells. Journal of cellular biochemistry **2004**;91(5):915-25 doi 10.1002/jcb.20008.
58. Ma M, Wang X, Ding X, Jing J, Ma Y, Teng J. Protective effect of BAG5 on MPP+-induced apoptosis in PC12 cells. Neurological research **2012**;34(10):977-83 doi 10.1179/1743132812y.0000000102.
59. Chaffer CL, Weinberg RA. A perspective on cancer cell metastasis. Science (New York, NY) **2011**;331(6024):1559-64 doi 10.1126/science.1203543.
60. Pearce OMT, Delaine-Smith RM, Maniati E, Nichols S, Wang J, Bohm S*, et al.* Deconstruction of a Metastatic Tumor Microenvironment Reveals a Common Matrix Response in Human Cancers. Cancer discovery **2018**;8(3):304-19 doi 10.1158/2159-8290.cd-17-0284.

Figure Legends

Figure 1. miR-4454 is a key microRNA downregulated in early and advanced OC metastasis. **(A)** Overview of the strategy for analysis of primary vs. metastatic OC patient tumor microRNA sequencing data and OC on organotypic 3D omental culture microRNA profiling. RNA isolated from frozen tumor tissue was used for microRNAseq. GFP-tagged OC cells (Kuramochi, OVCAR4 and OVCAR8) were grown on 3D omental culture for 48 h, isolated by FACS, RNA was isolated and microRNA expression was compared to the sham treated controls using NanoString. **(B)** Schematic representation of the organotypic omental 3D culture model. Mesothelial cells and fibroblasts were isolated from omentum obtained from female donors. The fibroblasts were mixed with type I collagen and seeded in a 10 cm dish. Once attached, they were overlaid with a confluent monolayer of mesothelial cells. Together they mimic the basement membrane and the mesothelium on the surface of the omentum. They were allowed to grow and for 24h so that the secreted factors from the cells could generate a complex microenvironment. Thereafter, GFP labeled OC cells (Kuramochi/OVCAR4/OVCAR8)

were seeded on the 3D omentum culture and allowed to grow. After 2 days, the OC cells were separated using fluorescence activated cell sorting (FACS) and used for RNA isolation and microRNA profiling with NanoString nCounter miRNA Expression Assay (800 microRNAs). Controls were seeded directly on the 10 cm culture dishes and were sham treated. **(C)** microRNA-target interaction networks for the 26 common downregulated microRNAs in patient metastasis and 3D omental culture using miRNet. microRNA hubs are depicted as blue dots and targets as red dots. **(D)** *Top:* qRT-PCR validation of miR-4454 in a set of OC patient primary and metastatic tumors. A line connects the expression data for each pair of primary and metastasis. *Bottom:* qRT-PCR validation of miR-4454 expression in OC cells (Kuramochi, OVCAR4 and OVCAR8) seeded on the 3D omental culture. * $p<0.01$, Students t-test. **(E)** OC cells isolated from ascites of 2 OC patients (ASC1 and 2) were grown on 3D omental culture for 48 h, separated by FACS and used for RNA isolation and qRT-PCR for miR-4454 expression. Mean ± SD from 3 independent experiments. * $p<0.01$, Students t-test. **(F)** Kaplan–Meier plot comparing patient survival when miR-4454 is upregulated or downregulated 1.5 fold in metastasis (Mets) vs. primary tumors in the OC patient cohort.

Figure 2. (A) Overexpression of miR-4454 inhibits motility and growth of OC cells. Kuramochi, OVCAR3, OVCAR4 and OVCAR8 cells were transfected with pre-miR-4454 or scrambled control oligos (Scr) and used for the functional assays. Migration: Transfected cells were seeded in transwell inserts with 8 µm pores and allowed to migrate towards medium containing 10% FBS. Migrated cells were fixed at the optimal time points, imaged and quantified using image-J software (mean ± SD; 3 independents experiments). Proliferation: Transfected cells were seeded in 96-well plates and allowed to grow for 5 days. Cell proliferation was determined by MTT assay (mean ± SD; 3 independents experiments). Colony formation: Transfected cells were seeded in 6-well plates for a colony formation assay. Once visible colonies were formed, the colonies were fixed, stained, imaged and counted using image-J software (mean ± SD; 3 independents experiments). **(B) Inhibition of miR-4454 increases the motility and growth of metastatic OC cells.** Kuramochi, OVCAR3, OVCAR4 and OVCAR8 cells were transfected with anti-miR-4454 or scrambled control oligos (Scr) and used for the migration, proliferation and colony formation assays as described above (mean ± SD; 3 independents experiments). * $p<0.01$, ** $p<0.05$, Students t-test. **(C) Invasion through the 3D omentum culture.** Schematic representation of the 3D invasion model

mimicking the invasion of metastasizing OC cells through the outer layers of the omentum. The 3D omentum culture was assembled in fluoroblock transwell inserts with 8 μm pores. GFP labeled OC cells were seeded on the 3D culture and allowed to invade though it towards the lower chamber containing medium with 10% FBS. **(D) Top:** Kuramochi and OVCAR4 cells were transfected with pre-miR-4454 or scrambled control oligo (Scr) and evaluated for their ability to invade through the 3D omental culture. Invasion was stopped at the optimal time. The invaded GFP labeled OC cells were imaged using the EVOS FL auto microscope and quantified using image-J software (mean ± SD; 3 independent experiments). **Bottom:** Kuramochi and OVCAR4 cells were transfected with anti-miR-4454 or scrambled control oligo (Scr) and their ability to invade through the 3D omental culture was evaluated. The invaded GFP cells were imaged and quantified using image-J software (mean ± SD; 3 independent experiments). Representative images of OC cells that have invaded through the 3D omentum culture, for each of these treatment groups are shown above respective graphs. **(E)**. OVCAR8 GFP cells transfected with scrambled control oligos, anti-miR-193b or pre-miR-193b, were seeded on 3D omental culture and allowed to form colonies. The fluorescent colonies were imaged on a Syngene G-Box imaging system and counted using image-J software (mean ± SD; 3 independents experiments). * $p<0.01$, Students t-test compared to control.

Figure 3. miR-4454 inhibits OC metastasis *in vivo.* OVCAR8 cells stably overexpressing miR-4454 were generated using a lentiviral pre-miR-4454 vector. The effect of stable expression of miR-4454 in OVCAR8 cells on their ability to form metastasis in mouse xenografts was tested by injecting $5x10^6$ cells intraperitoneally in female, athymic nude mice and compared to vector controls. Mice were euthanized after 35 days and the peritoneal metastasis were counted, surgically resected and weighed. **(A)** Graphical representation of the number of metastasis. **(B)** Graphical representation total tumor weight of OVCAR8 tumors stably expressing miR-4454 compared to control vector (mean ± SD; n=10 mice/group; *$p<0.01$). **(C)** Representative images of the peritoneal metastasis in each group with the tumors outlined in black **(D)** Validation of miR-4454 overexpression in the omental tumors. Omental tumors (n=3/group) were homogenized, RNA was isolated, and qRT-PCR was performed for miR-4454. **(E)** FFPE tumor sections (n=5/group) were stained for cleaved caspase-3. A representative image is shown (left) and the quantification of the cleaved caspase-3 staining is plotted (right).

(F) *Left:* Representative images of FFPE tumor sections (n=5/group) stained for Ki-67. *Right:* The quantification of the Ki-67 staining (mean ± SD; *p<0.01, Students t-test).

Figure 4. Microenvironmental regulation of miR-4454. (A) GFP-tagged Kuramochi cells were seeded on a confluent monolayer of human primary mesothelial cells (HPMC), normal omental fibroblasts (NOF) and cancer associated fibroblasts (CAF) for a period of 48 h. Thereafter, the Kuramochi cells were separated by FACS, RNA was isolated and qRT-PCR was performed for the expression of miR-4454. A significant reduction in miR-4454 expression was observed upon coculture with NOFs and CAFs (mean ± SD from 3 independent experiments). **(B)** Kuramochi cells were grown in condition medium (CM) collected from normal omental fibroblasts (NOF) or cancer associated fibroblasts (CAF) isolated from OC patients. qRT-PCR was done to test the effect on expression of miR-4454 in OC cells grown on CM compared with corresponding controls grown in serum free medium. **(C):** Proximal culture overview. **Step 1** OC cells were seeded on the lower surface of a transwell insert with 0.4μm pores and allowed to attach. **Step 2** Then the insert was flipped and placed in a well containing growth medium. **Step 3** The fibroblasts were seeded on the upper surface of the insert and the two cell types were allowed to grow in close proximity of each other but separated by a 10μm thick membrane having 0.4μm pores. This allowed the dynamic exchange of paracrine factors (magnified inset) at localized high concentrations while inhibiting juxtacrine signaling. **(D)** Kuramochi cells in proximal culture with NOFs, CAFs or dermal fibroblasts (D.Fibroblast) for 48 h were used for RNA isolation and qRT-PCR for miR-4454 expression compared corresponding controls, which did not have the fibroblasts seeded on the opposite surface. Mean ± SD from 3 independent experiments; * p<0.01, Students t test.

Figure 5. Identification of miR-4454 targets. (A) RNAseq was done on Kuramochi and OVCAR4 cells transfected with pre-miR-4454 or scrambled control oligos (n=3/group). Venn diagram showing the number of genes uniquely and commonly downregulated in Kuramochi and OVCAR4 cells overexpressing miR-4454 compared to the respective controls. **(B)** The 811 common downregulated genes were analyzed for predicted miR-4454 seed matches in their 3'UTR using microRNA target prediction software TargetScan, miRDB and TargetMiner. Heat map showing the extent of downregulation of the 68 genes, with predicted miR-4454 seed matches, in miR-4454 overexpressing

Kuramochi and OVCAR4 cells compared to the corresponding controls. **(C)** qRT-PCR validation of selected targets in OC cells overexpressing miR-4454. qRT-PCR for SPARC, BAG5 and SOX4 was done using RNA from Kuramochi and OVCAR4 cells transfected with pre-miR-4454 or scrambled control oligos. The baseline SOX4 expression was too low and it was not detected. (mean ± SD from 3 independent experiments). * $p<0.01$, ** $p<0.05$, Students t-test. **(D)** 3'UTR luciferase reporter assay for the binding of miR-4454 to the 3'UTR of BAG5 or SPARC. Wild type (WT) or miR-4454 seed match mutated (Mut) BAG5 or SPARC 3'UTR luciferase constructs were co-transfected with pre-miR-4454 (pre-4454) or scrambled control (Scr) in 293T cells, the conditioned medium collected, and the secreted gaussia luciferase and alkaline phosphatase activity was measured. Luciferase activity was normalized to the alkaline phosphatase activity for transfection normalization (mean±SD; 3 independent experiments). **(E-F)** Functional effects of miR-4454 targets. Kuramochi, OVCAR4 and OVCAR8 cells were transfected with BAG5 siRNA **(E)** or SPARC siRNA **(F)** or scrambled control oligo (Scr) and the effects of silencing them were evaluated on the ability of the cells to migrate, proliferate and form colonies. **(E) and (F)** *left panel - Migration*: Transfected cells were seeded in transwell inserts with 8 µm pores in and allowed to migrate towards medium containing 10% FBS in the lower chamber. Migrated cells were fixed, imaged and quantified using image-J software (mean ± SD; 3 independents experiments). Representative images of migrated cells are provided over each treatment group. **(E)** and **(F)** *middle panel - Proliferation*: Transfected cells were seeded in 96-well plates and allowed to grow for 5 days. Cell proliferation was determined by MTT assay (mean ± SD; 3 independents experiments). **(E) and (F)** *right panel - Colony formation*: Transfected cells were seeded in 6 well plates and allowed to form colonies. Colonies were fixed after 2-3 weeks, stained (0.005% crystal violet) and counted using image-J software (mean ± SD; 3 independents experiments). Representative images of colonies are provided. * $p<0.01$, Students t-test.

Figure 6. Functional rescue experiments to test if BAG5 and SPARC are direct downstream effectors of miR-4454. Kuramochi cells were transfected with anti-miR-4454/BAG5-siRNA/SPARC-siRNA or both anti-miR-4454 and siRNA or scrambled control oligos (Scr). The transfected cells were then used for the functional assays. **(A)** Migration: Transfected cells were seeded in transwell inserts with 8 µm pores in and allowed to migrate towards medium containing 10% FBS. Migrated cells were fixed,

imaged and quantified using image-J software (mean ± SD; 3 independents experiments). **(B)** Transfected cells were seeded in 96-wella plates and allowed to grow for 5 days. Cell proliferation was determined by MTT assay (mean ± SD; 3 independents experiments). **(C)** Colony formation: Transfected cells were seeded in 6-well plates and allowed to form colonies. Colonies were fixed after 2-3 weeks, stained (0.005% crystal violet) and counted using image-J software (mean ± SD; 3 independents experiments). * $p<0.01$, Students t-test. **(D)** Kaplan–Meier plot for effect of BAG5 (Affy ID:202985_s_at) and SPARC (Affy ID: 212667_at) expression levels on 5-year progression free survival in ovarian cancer patients using KM Plotter. Red: High expression; Black: Low expression.

Figure 7. Mechanism of action of miR-4454 through BAG5 and SPARC. (A) The OC cells (OVCAR3, OVCAR4 and Kuramochi) were transfected with pre-miR-4454 or scrambled control oligo (Scr) (*left panel*) or with BAG5 siRNA or scrambled control oligos (Scr) (*right panel*). Cells were allowed to grow for 48 h and then lysed in RIPA buffer. Proteins were separated by 4-20% gradient SDS-PAGE and transferred to nitrocellulose membrane, probed with BAG5, cleaved PARP, cleaved caspase-3 and p53 antibodies. Representative blots from 3 independent experiments are shown. **(B)** OVCAR3, OVCAR4 or Kuramochi cells were transfected with pre-miR-4454 or scrambled control oligo (Scr) (*left panel*) or with SPARC siRNA or scrambled control oligos (Scr) (*right panel*). Cells were allowed to grow for 48 h and then lysed in RIPA buffer. Proteins were separated by 4-20% gradient SDS-PAGE and transferred to nitrocellulose membrane, probed with SPARC, phosphorylated FAK at Tyr397 (pFAK) and total FAK antibodies. Representative blots from 3 independent experiments are shown. **(C)** Schematic overview of findings. Paracrine signals from microenvironmental fibroblasts lead to downregulation of miR-4454 in metastasizing OC cells. The downregulation of miR-4454 promotes metastatic colonization through the concomitant increased expression of its targets SPARC and BAG5, which help by activating FAK, promoting mutant p53 gain of function by its stabilization and inhibiting apoptosis respectively.

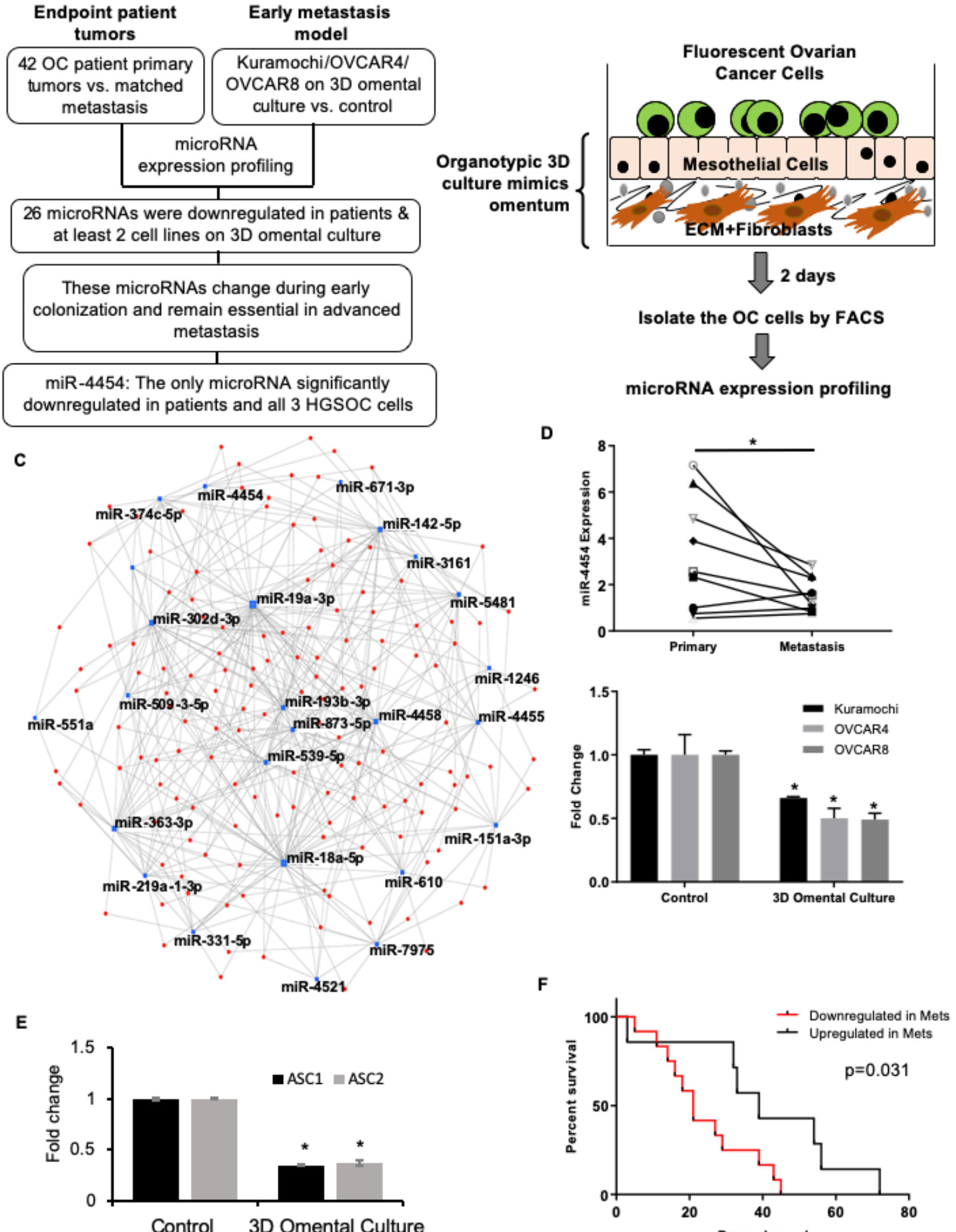

Author Manuscript Published OnlineFirst on April 29, 2020; DOI: 10.1158/1541-7786.MCR-19-1162
Author manuscripts have been peer reviewed and accepted for publication but have not yet been edited.

Figure 2

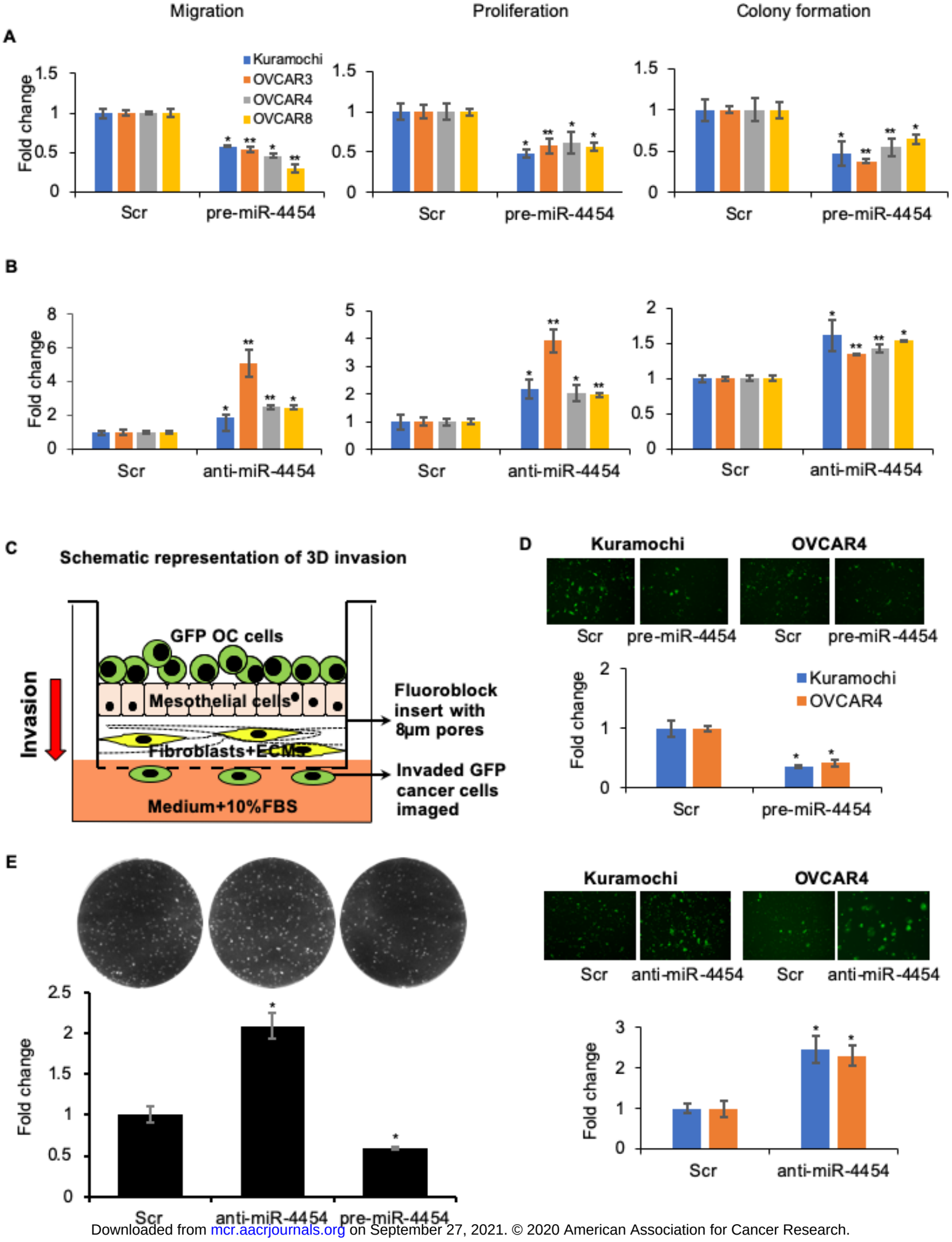

Author Manuscript Published OnlineFirst on April 29, 2020; DOI: 10.1158/1541-7786.MCR-19-1162
Author manuscripts have been peer reviewed and accepted for publication but have not yet been edited.

Figure 3

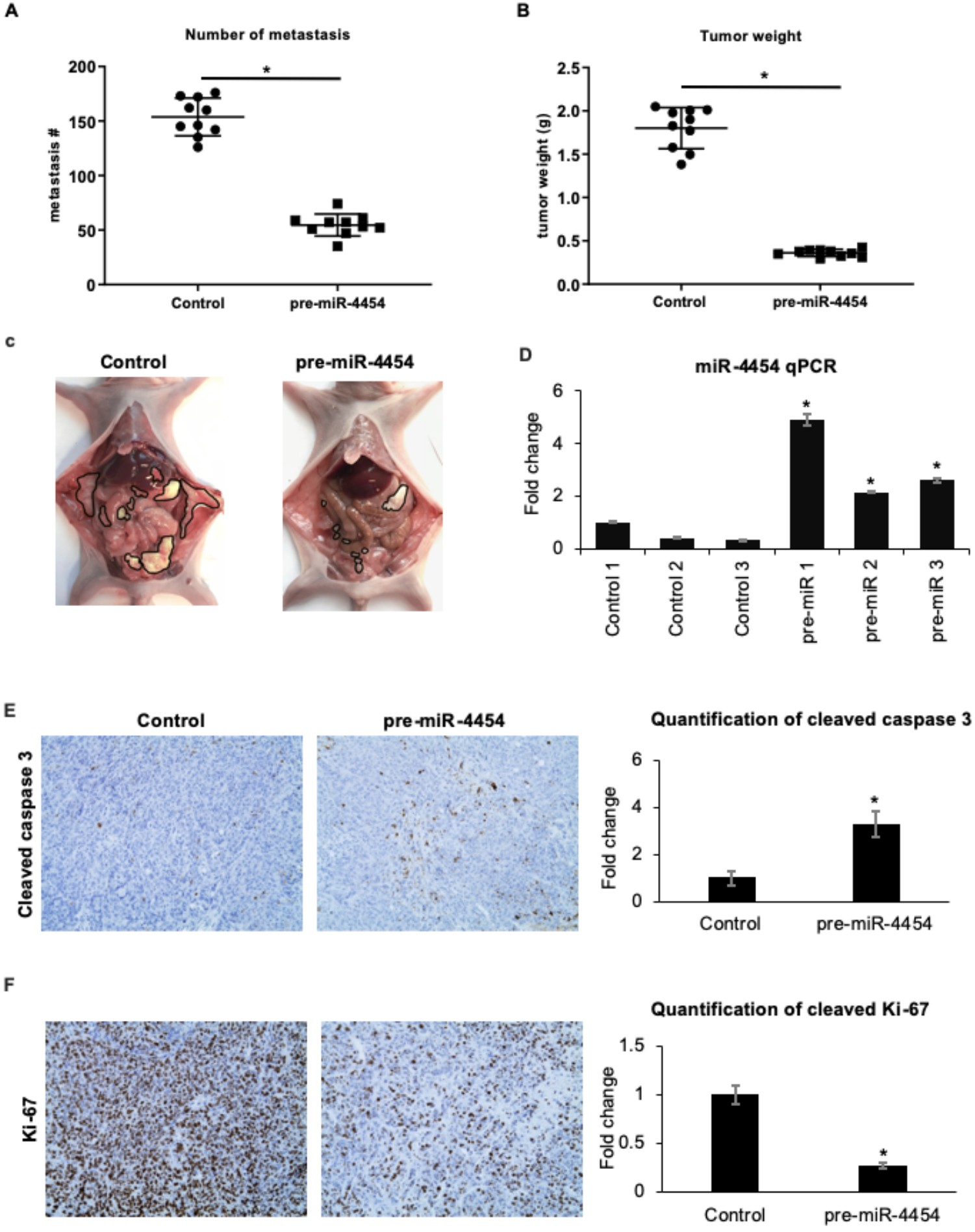

Author Manuscript Published OnlineFirst on April 29, 2020; DOI: 10.1158/1541-7786.MCR-19-1162
Author manuscripts have been peer reviewed and accepted for publication but have not yet been edited.

Figure 4

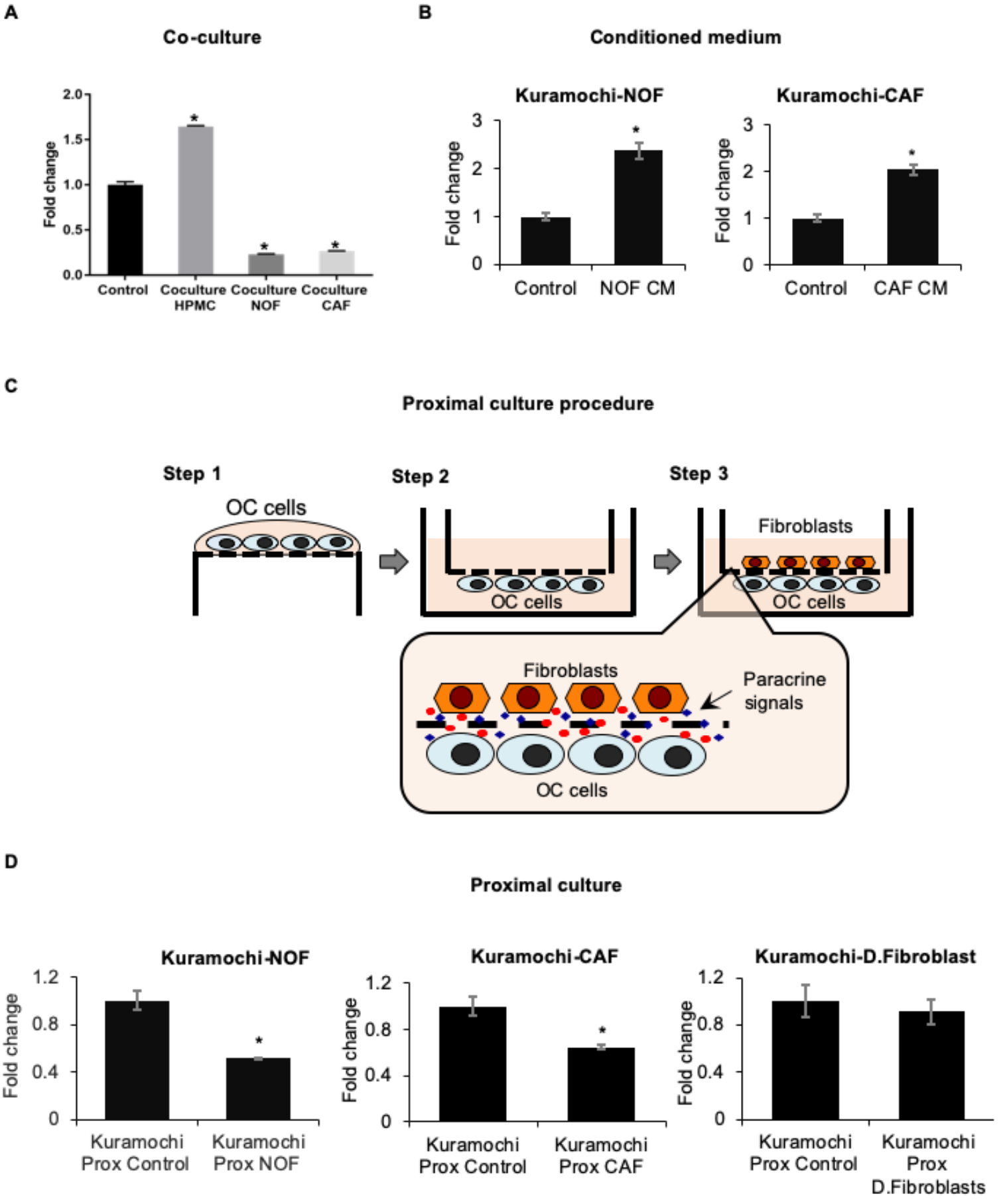

Author Manuscript Published OnlineFirst on April 29, 2020; DOI: 10.1158/1541-7786.MCR-19-1162
Author manuscripts have been peer reviewed and accepted for publication but have not yet been edited.

Figure 5

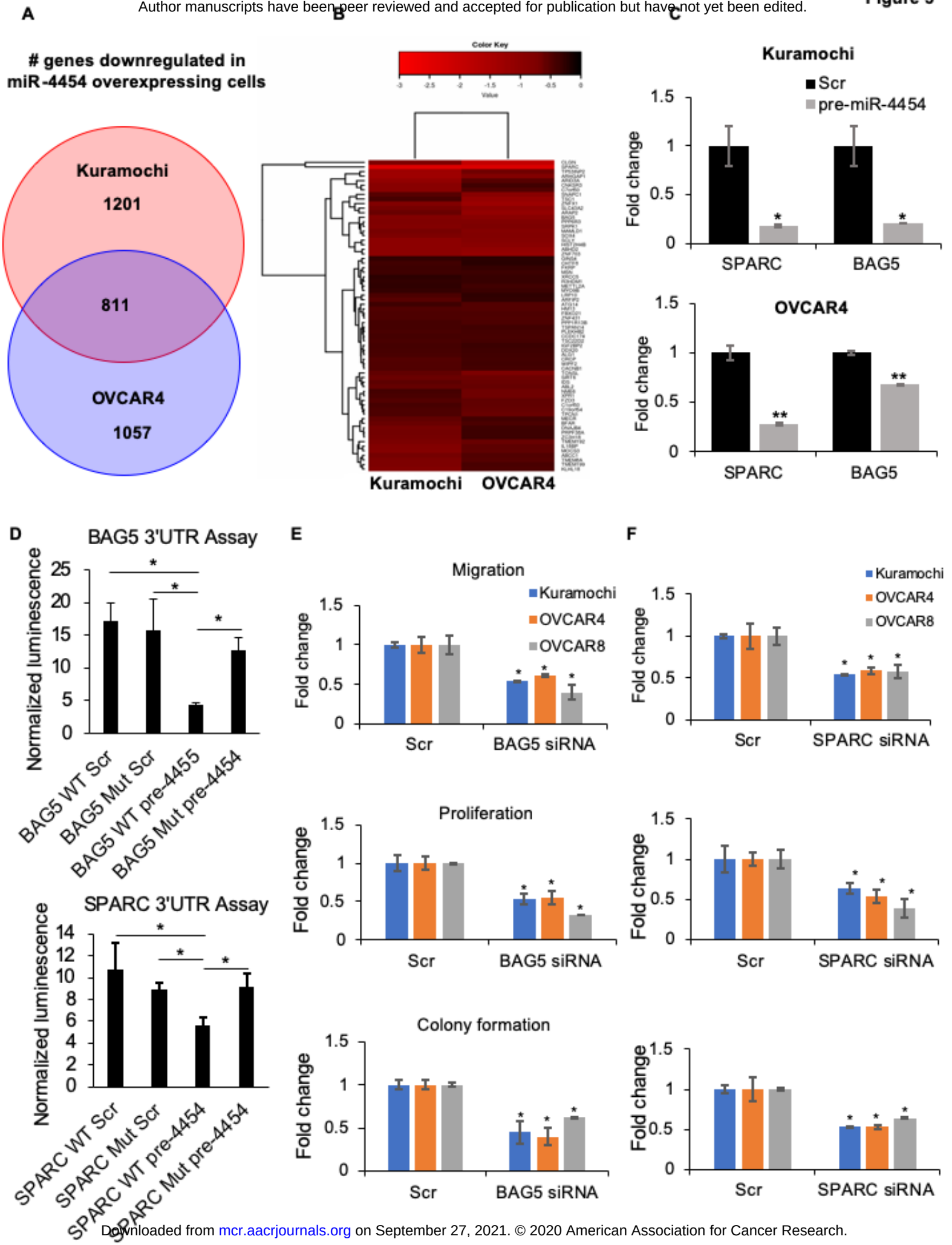

Figure 6

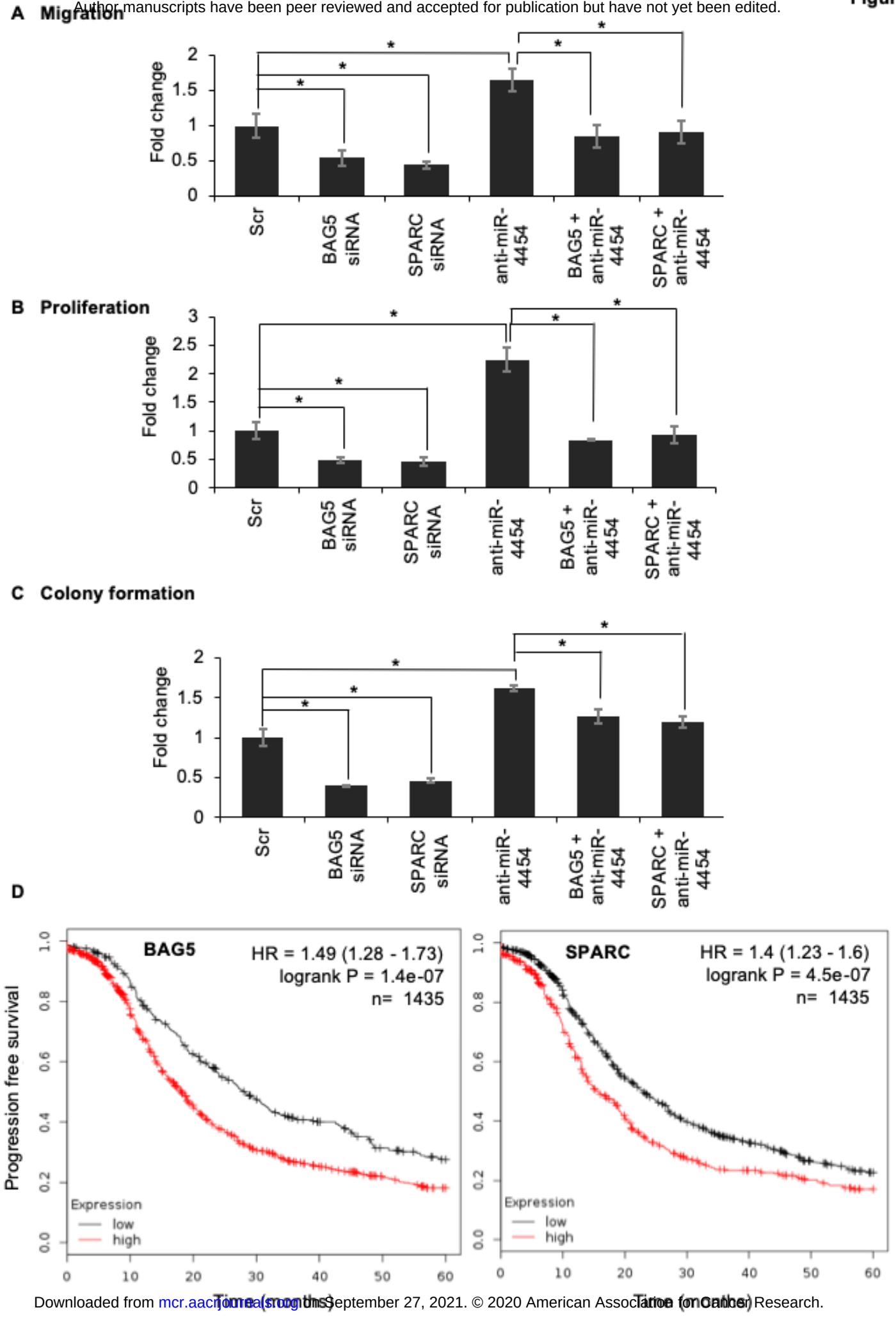

Author Manuscript Published OnlineFirst on April 29, 2020; DOI: 10.1158/1541-7786.MCR-19-1162
Author manuscripts have been peer reviewed and accepted for publication but have not yet been edited.

Figure 7

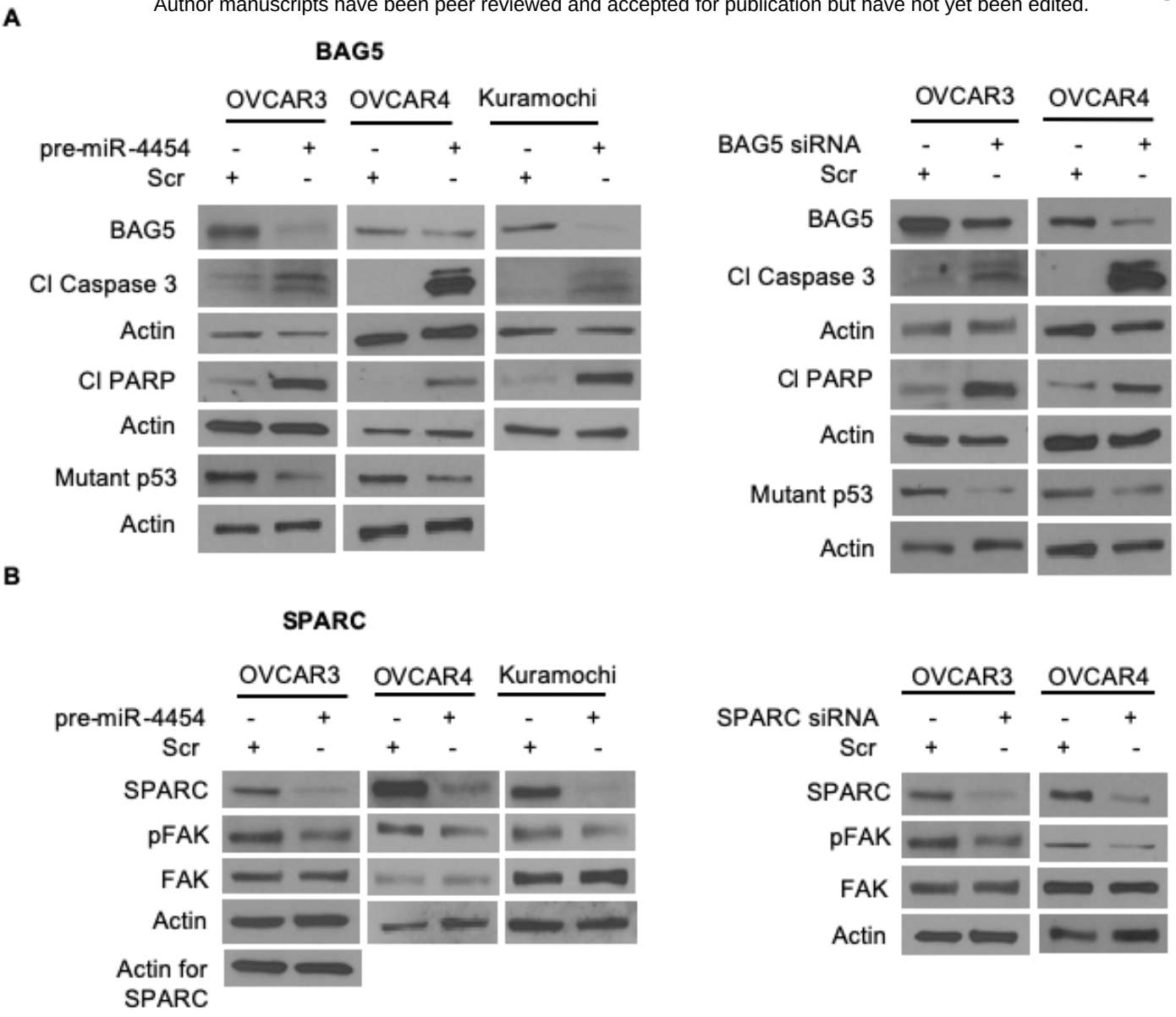

AACR American Association for Cancer Research

Molecular Cancer Research

Signals from the metastatic niche regulate early and advanced ovarian cancer metastasis through miR-4454 downregulation

Subramanyam Dasari, Taruni Pandhiri, Tommaso Grassi, et al.

Mol Cancer Res Published OnlineFirst April 29, 2020.